Properties of knotted ring polymers. I. Equilibrium dimensions

ARTICLE *in* THE JOURNAL OF CHEMICAL PHYSICS · JULY 2010

Impact Factor: 2.95 · DOI: 10.1063/1.3457160 · Source: PubMed

2 AUTHORS:

Marc L Mansfield
Utah State University
85 PUBLICATIONS **1,973** CITATIONS
SEE PROFILE

J. F. Douglas
National Institute of Standards and Technolo…
428 PUBLICATIONS **14,795** CITATIONS
SEE PROFILE

Properties of knotted ring polymers. I. Equilibrium dimensions

Marc L. Mansfield[1,a),b)] and Jack F. Douglas[2,a),c)]
[1]*Department of Chemistry, Chemical Biology, and Biomedical Engineering, Stevens Institute of Technology, Hoboken, New Jersey 07030, USA*
[2]*Polymers Division, National Institute of Standards and Technology, Gaithersburg, Maryland 20899, USA*

(Received 27 January 2010; accepted 3 June 2010; published online 27 July 2010)

We report calculations on three classes of knotted ring polymers: (1) simple-cubic lattice self-avoiding rings (SARs), (2) "true" theta-state rings, i.e., SARs generated on the simple-cubic lattice with an attractive nearest-neighbor contact potential (θ-SARs), and (3) ideal, Gaussian rings. Extrapolations to large polymerization index N imply knot localization in all three classes of chains. Extrapolations of our data are also consistent with conjectures found in the literature which state that (1) $R_g \to AN^{\nu}$ asymptotically for ensembles of random knots restricted to any particular knot state, including the unknot; (2) A is universal across knot types for any given class of flexible chains; and (3) ν is equal to the standard self-avoiding walk (SAW) exponent ($\cong 0.588$) for all three classes of chains (SARs, θ-SARs, and ideal rings). However, current computer technology is inadequate to directly sample the asymptotic domain, so that we remain in a crossover scaling regime for all accessible values of N. We also observe that $R_g \sim p^{-0.27}$, where p is the "rope length" of the maximally inflated knot. This scaling relation holds in the crossover regime, but we argue that it is unlikely to extend into the asymptotic scaling regime where knots become localized. © *2010 American Institute of Physics*. [doi:10.1063/1.3457160]

I. INTRODUCTION

Ring polymers exist in specific knot states that cannot be altered without breaking bonds. Most theoretical predictions about ring polymers apply to ensembles that include all possible knot states. However, because ring-closure reactions can occur far from equilibrium, such results may not be directly applicable. We illustrate this point in relation to the scaling laws for the average polymer size (radius of gyration),

$$R_g \sim N^{\nu_{\mathrm{SAR}}}, \quad \nu_{\mathrm{SAR}} \cong 0.588 \tag{1a}$$

or

$$R_g \sim N^{\nu_{\mathrm{IR}}}, \quad \nu_{\mathrm{IR}} = 0.5, \tag{1b}$$

which hold in the limit of long chains for self-avoiding ring (SAR) and ideal ring (IR) ensembles, respectively, that include all possible knot states. There is no obvious reason to expect ensembles confined to a single knot type to obey the same scaling laws. The N-dependence of R_g for such ensembles is the primary focus of this paper. We present Monte Carlo data on three types of ring ensembles: (1) simple-cubic lattice SAR knots to model ring polymers in good-solvent or swollen conditions; (2) simple-cubic lattice theta-state rings (θ-SARs), i.e., SARs with an attractive nearest-neighbor contact potential to model poor-solvent conditions; and (3) ideal, Gaussian chains. Figure 1 displays projections of all of the knot states examined in this study. Ideal chains are of course only an idealization of the poor-solvent regime, and for all we know, this model may be unrealistic for representing topological properties of real polymers in solution.[1] To the best of our knowledge, the current study is the first to examine knotting in the "true" theta-state, i.e., chains for which the segmental interaction includes both repulsive excluded volume and attractive poor-solvent contributions.

Evidence is accumulating that large SARs at equilibrium display a phenomenon known as knot localization.[2–8] Apparently, if any given prime knot is present in a sufficiently large SAR then the most probable conformations are those for which the knot is localized in some part of the ring, rather than being spread out throughout the ring. For composite knots, each prime factor appears to be localized independently in some part of the chain. This phenomenon is closely related to a similar effect seen in "paraknots," or chains confined to pass through "slip links," as in Fig. 2.[9–14] The theta-point appears to be the transition between knot localization and delocalization,[5,15] so that the effect is expected to be weaker in IRs than in SARs. However, knot localization is well established in ideal paraknots,[9–12] and in this work, we find evidence for it in SARs, θ-SARs, and IRs.

A related question concerns the prevalence of knotting in ring polymers. In this case, we ask for the probability that the elements of some particular ensemble of rings, for example, SARs of a given length, are found in a particular knot state. It was conjectured by Frisch and Wasserman,[16] and independently by Delbrück,[17] that very long chains are almost always knotted. A number of separate proofs of the Frisch–Wasserman–Delbrück (FWD) conjecture have appeared.[18–23] (It seems necessary to construct an independent proof for each particular ensemble that might be considered.) All of these are essentially variants of the Kesten pattern theorem, which asserts that any given pattern which can occur in a random sequence, will occur if the sequence is sufficiently

a)Authors to whom correspondence should be addressed.
b)Electronic mail: marc.mansfield@stevens.edu.
c)Electronic mail: jack.douglas@nist.gov.

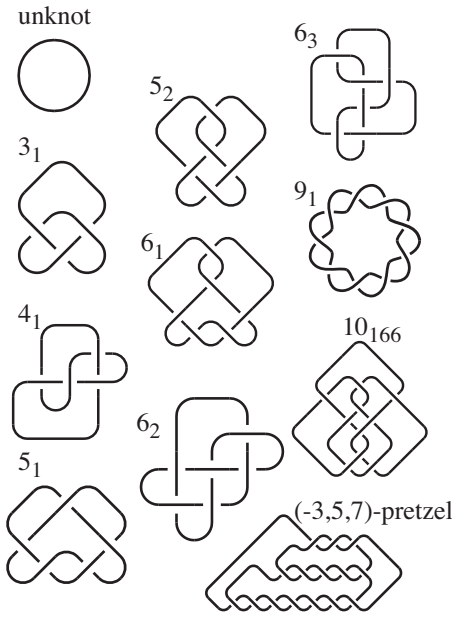

FIG. 1. The knot states considered in this work.

long. Therefore, a corollary to the FWD conjecture is that knot complexity increases with ring size. The FWD conjecture has been abundantly verified in Monte Carlo calculations, which also indicate that the prevalence of knotting depends on the nature of the ensemble.[20,24–41] For example, SARs on the simple-cubic lattice become knotted only when extremely long. Knotting increases as we progress through the theta-point into the collapsed chain domain. One way of characterizing this behavior is to specify the value of the chain length, N_U, for which the unknot probability falls to $1/e$. For SARS on the simple-cubic lattice, N_U is around 10^5-10^6, while at the theta-point it drops to about 10^4.[42] For collapsed chains, N_U is on the order of a few hundred.[42] Knotting has also been investigated in lattice Hamiltonian paths as models of collapsed polymers, and these are also copiously knotted when N is larger than about 100.[43,44] (However, Ref. 43 is the only study of Hamiltonian paths to have achieved unbiased sampling.[45]) In the following, we will refer to ensembles satisfying $N \ll N_U$ and $N \gg N_U$, respectively, as being unknot-dominant or unknot-depleted.

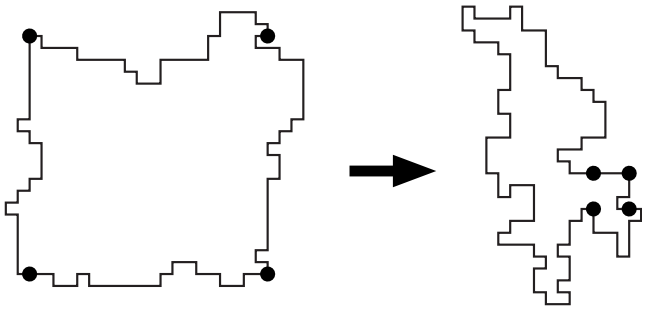

FIG. 2. Localization effects in a "paraknot," or a ring polymer constrained to visit the four corners of a square of side s. For large s, the most-probable distribution corresponds to a symmetric distribution of segments among the four loops. However, at small s, the symmetry is broken, and the most-probable distribution assigns a large majority of segments to one of the loops. The paraknot has become localized in a small part of the ring.

TABLE I. Characteristics of the knots studied in this work. C=minimum crossing number, X=average crossing number of the maximally inflated knot, p="ropelength" of the maximally inflated knot, and $n_{\min}$=minimum number of steps required for the knot on the simple-cubic lattice.

	C	X [a]	p [a]	$7.11C^{0.768}$	$n_{\min}$ [b]
Unknot	0	0	3.14	0	4
3_1	3	4.26	16.33	16.5	24
4_1	4	6.47	20.99	20.6	30
5_1	5	7.75	23.55	24.5	34
5_2	5	8.21	24.68	24.5	36
6_1	6	10.15	28.30	28.2	40
6_2	6	10.39	28.47	28.2	40
6_3	6	10.52	28.88	28.2	40
9_1	9	15.18	37.81	38.4	54
10_{166}	10	18.54	41.52	41.7	56
"Pretzel"	15	24.7	51.8	56.9	74[c]

[a]References 46 and 49–51.
[b]References 75 and 76.
[c]Determined by us.

It has been argued[46] that many properties of general knots having arbitrary conformations can be related to the properties of one rather special conformation, the "maximally inflated" or "ideal" knot.[47] Imagine a knot modeled as a rope with finite thickness d and with contour length L. Then imagine transforming the structure either by increasing d at constant L ("inflating" the knot)[2] or by decreasing L at constant d.[48] The maximally inflated knot is that structure for which, for a given knot type, the ratio L/d achieves its global minimum. We also let p, the "rope length," represent the value of this global minimum: $p=[L/d]_{\min}$. Other properties of knots are the so-called minimum crossing number C and average crossing number X. C is the smallest possible number of crossings with which a projection of the knot can be drawn. For example, Fig. 1 displays all of the knot types considered in this work, and each is drawn with the minimum number of crossings. The average crossing number X is obtained from the maximally inflated conformation, and is the mean number of crossings when averaged over all possible orientations. Values of p, C, and X for many knots are tabulated in Refs. 46 and 49, while several other values were communicated to us privately.[50,51] The values for all the knots of Fig. 1 are reproduced in Table I.

We now demonstrate that as a general rule, R_g for a single knot type varies more strongly with N than it does for an ensemble containing all possible knot types. (See Ref. 52 for a similar, nonquantitative argument.) First, we assume that we have some quantitative, real-valued knot invariant which serves as a measure of entanglement complexity.[19] Properties such as C,X,p, or real numbers derived from nonreal invariants (span of a knot polynomial,[53] for example) are probably all adequate for the present argument. Let the symbol Z represent the ensemble average of this invariant. For an ensemble containing all possible knot types we expect Z to increase with N. This is essentially a restatement of the FWD conjecture cited above. We also expect a negative correlation between Z and R_g, since on average, a polymer ring found in a more complex knot state will display more self-entanglement and have a smaller coil size. We write

$$dR_g = \rho dN - \sigma dZ \tag{2}$$

to represent the change in R_g resulting from changes in N and in Z, where R_g is the rms ensemble-average radius of gyration. As already asserted, we expect a positive correlation between R_g and N, and a negative correlation between R_g and Z, so as defined by Eq. (2), ρ and σ are both positive. Then,

$$\left(\frac{\partial R_g}{\partial N}\right)_Z = \rho \tag{3}$$

and

$$\frac{\partial R_g}{\partial N} = \rho - \sigma \frac{\partial Z}{\partial N}, \tag{4}$$

where Eq. (3) represents the rate of growth in R_g at fixed knot complexity, or similarly, for an ensemble of fixed knot type, while Eq. (4) represents the rate of growth for ensembles not restricted to knot type. As already mentioned, $\partial Z/\partial N > 0$. Therefore, we can write

$$\left(\frac{\partial R_g}{\partial N}\right)_Z > \frac{\partial R_g}{\partial N}, \tag{5}$$

which establishes that R_g for a single knot type is a stronger function of N than R_g for an unrestricted ensemble.

The inequality of Eq. (5) would obviously be satisfied if the asymptotic metric exponent of an ensemble confined to a specific knot type was greater than the exponent for an unrestricted ensemble. Nevertheless, it has been argued that the asymptotic exponent for any SAR ensemble restricted to a single knot type is still ν_{SAR}.[2,8,54–56] This is not inconsistent with Eq. (5), since the inequality can be entirely satisfied by the nonasymptotic behavior. On the other hand, it has been argued that when ensembles of IRs are confined to one particular knot type, the asymptotic exponent is also exactly ν_{SAR}.[52,57–60] This argument is based on the assertion that the topological constraints which confine the polymer to one particular knot type are effectively equivalent to segmental repulsion.[58] Obviously, this argument also satisfies the inequality of Eq. (5). Interestingly, what appear to be the most widely believed assertions in the literature are that when passing from a unrestricted ensemble to a subensemble restricted to a single knot type, the asymptotic exponent does not change for SARs while it does for IRs.

There is no direct evidence for the above assertions concerning metric exponents, if by direct evidence we mean Monte Carlo data that directly display the anticipated exponents. Rather, all the available Monte Carlo data to date indicate very slow convergence, and it is doubtful that our current technology permits us to adequately sample the asymptotic domain. However, in a number of cases, existing Monte Carlo data have been fitted to scaling laws with finite-N corrections, such as the following expression:[8,33,52,54,61–63]

$$R_g = AN^{\nu}[1 + BN^{-\Delta} + \cdots]. \tag{6}$$

In the case of SARs confined to a specific knot type, these fits suggest that $\nu \cong \nu_{\mathrm{SAR}}$ independent of the knot type (at least to within confidence limits of the fit), and also suggest that the amplitude A is independent of knot type. In the case of IRs the data are perhaps not quite so conclusive. Nevertheless, a number of workers have presented evidence that the correct metric exponent is again ν_{SAR}.[8,52,59,60] Our results also fail to reach the asymptotic regime and are therefore not entirely conclusive, but for both SARs and θ-SARs, we find consistency with Eq. (6). Our data also suggest that A and ν are independent of knot type, and that $\nu \cong \nu_{\mathrm{SAR}}$ for both SARs and θ-SARs.

Since $N \ll N_U$ corresponds to unknot dominance of unrestricted ensembles, we expect any ensembles that are restricted to unknots to be practically indistinguishable from unrestricted ensembles, and therefore to follow either Eq. (1a) or Eq. (1b) at such values of N. This also implies that if Eqs. (1) are not asymptotically correct for ensembles of unknots, then the crossover to asymptotic behavior will occur no sooner than when the distinction between the two ensembles first occurs, or no sooner than $N \approx N_U$. We should also be open to the possibility that N_U determines the position of crossover to asymptotic behavior for other knots as well. Since N_U is so large]($\approx 10^{5.5}$ and $\approx 10^4$, respectively, for SARs and θ-SARs (Ref. 42)] direct verification of the behavior of R_g near N_U is not currently possible.

Knot localization appears to be directly related to the asymptotic scaling of ensembles of fixed knot type. If the knot is confined to a subsection of length N_K, and if, as now appears likely, we have $\langle N_K \rangle / N \to 0$ in the long-chain limit, then the chain can be replaced with an effectively unknotted ring of length $N - N_K \cong N$, which would imply that the asymptotic metric exponent ν and the amplitude A for any particular knot is the same as that for the unknot.[6,8] If, as some have proposed, we have $\langle N_K \rangle \sim N^t$ with $t < 1$, then we would have[5,64]

$$R_g = A(N - bN^t)^{\nu}, \tag{7}$$

which agrees well with Eq. (6) if we take $\Delta = 1 - t$ and $B = -b\nu$. As reported below, our data are consistent with the phenomenon of knot localization in SARs, theta-SARs, and IRs, and therefore support the argument that ν and A are independent of knot type.

By constructing Flory arguments for knotted SARs, Quake[55] and Grosberg *et al.*[2] have respectively obtained the following scaling laws:

$$R_g \sim N^{3/5} C^{-4/15}, \tag{8}$$

$$R_g \sim N^{3/5} p^{-4/15}. \tag{9}$$

Equations (8) and (9) depend on the respective assumptions that a knot consists of C loops of length N/C each,[55] or that the maximally inflated knot is a primitive path[65] for the solvated coil. (The two arguments are closely related, being based on the respective assumptions that either C or p defines a renormalized chain length.) Of course, neither of these assumptions is tenable given the phenomenon of knot localization. Furthermore, Eqs. (8) and (9) imply $A \sim C^{-4/15}$ and $p^{-4/15}$, respectively, and are therefore incompatible with the assertion that A is independent of knot state. One way out of this impasse would be to assert that $C^{-4/15}$ or $p^{-4/15}$ scaling is nonasymptotic, disappearing at very long chain lengths when knots become well localized. In this study we examine

our data for consistency with both Eqs. (8) and (9). At least for the knots and chain lengths studied, the p-dependence appearing in Eq. (9) is verified.

II. SIMULATION TECHNIQUES

In this work, we have modeled polymer rings as closed paths on the simple-cubic lattice. Excluded volume interactions are enforced by disallowing double occupancy of any given lattice site, and solvent quality is modeled through the strength of an attractive nearest-neighbor pair potential, $-\Phi$. In other words a Hamiltonian H is defined for each ring on the lattice, such that $H=\infty$ for any chain for which any two segments lie at the same lattice site, while for all other chains, $H=-n\Phi$, where n is the total number of pairs of nonsequential segments occupying neighboring lattice sites. We concentrate on two classes of ensembles, "swollen" rings, for which $\Phi=0$, and "theta" rings, at $\Phi=0.27$, the theta point of simple-cubic lattice chains.[42,66] Chain ensembles were prepared by the BFACF algorithm with Metropolis bias,[67–69] which is known to be ergodic in any given knot class.[70] This algorithm operates in the grand canonical ensemble, and we employ a chain length bias guaranteeing that the equilibrium probability of chains of length N is proportional to the total number of chains on the lattice at that chain length, which of course means that unchecked, chains would grow without limit. Therefore, we include one more term in the Hamiltonian. We take N_0 to be the nominal chain length of the ensemble, and the Hamiltonian of any chain for which $N>N_0$ contains the additional term $(N-N_0)^2$. The effect of this additional term is to produce a practically monodisperse chain length distribution, with all chains satisfying $N\cong N_0$. In summary, the complete Hamiltonian of any one realization of the chain is written

$$H = H_X(m) - n\Phi + H_L(N,N_0). \tag{10a}$$

Here, m equals the number of pairs of segments occupying identical lattice sites, n equals the number of pairs of segments lying at nearest-neighbor sites (not counting sequential segments along the chain), N is the actual chain length, and N_0 is the nominal chain length of the ensemble, and we have

$$H_X(m=0)=0, \quad H_X(m>0)=\infty, \tag{10b}$$

$$H_L(N\le N_0)=0, \quad H_L(N>N_0)=(N-N_0)^2. \tag{10c}$$

For the most part, we have examined N_0 values between 100 and 2000, although for several knot states, chain lengths as large as 10 000 have also been studied. Our ensembles for investigating knot-localization usually consisted of 200 specimens (300 for the theta-state chains). For values of $N_0 \le 2000$ successive specimens were completely annealed between samples, which was verified by monitoring radius-of-gyration correlations during the annealing process. At $N_0=10\,000$, complete annealing between samples is impractical. In this case, annealing times between samples were about an order of magnitude smaller than the radius-of-gyration correlation time, but the sampled ensembles consisted of 1200 specimens. (We concluded that the R_g data at $N_0=10\,000$ are probably compromised by sampling error, and so will not be reported. However, the knot localization results at $N_0=10\,000$ are given below.) Root-mean-square R_g values were computed concurrently, during the generation of both the knot-localization samples as well as the samples used to study transport properties, as reported in the companion paper.

We employed a technique first described by Deguchi and Tsurusaki[29] to generate ideal Gaussian rings. It has the advantage that subsequent rings are uncorrelated, so there is no need for annealing. However, these occur in all possible knot states, and so the knot state of each individual ring was determined using a recently developed procedure[71] based on recognition of the knot group.[72]

III. KNOT TYPES EXAMINED IN THIS STUDY

Eleven different knot types were examined in this study, as shown in Fig. 1. These are the unknot; the seven prime knots of six or fewer crossings, namely, 3_1 (also known as the "trefoil" knot), 4_1, 5_1, 5_2, 6_1, 6_2, and 6_3; the order-9 torus knot, 9_1; the knot 10_{166} (which is the last knot appearing in Rolfsen's tabulation[73] of all the primes of 10 or fewer crossings); and the $(-3, 5, 7)$-pretzel knot, Fig. 6.25 of Ref. 53, which is famous for having a trivial Alexander polynomial, and which will be referred to hereafter simply as the "pretzel." The characteristics of the maximally inflated forms of these knots, obtained from the literature,[46] the internet,[49] or by private communication,[51,50] are given in Table I.

Another knot characteristic is $n_{\min}$, the smallest number of segments needed to form a particular knot on the simple-cubic lattice, or in other words, the lattice equivalent of p. One reason for our interest in $n_{\min}$ is that it determines the lower bound to the size of a localized knot. The values $n_{\min}=4$ and $n_{\min}=24$ are known to be exact for unknots and trefoils, respectively.[74] Janse van Rensburg and Promislow[75] and Scharein *et al.*[76] tabulated $n_{\min}$ values that they obtained by simulated annealing, which probably, but not necessarily, achieves the global minimum. These values also appear in Table I.

Interestingly, for the eight knots between 3_1 and 9_1 in Table I, we have

$$p = 7.11C^{0.768}, \tag{11}$$

with errors of 4% or less. We do not want to imply that this is a general scaling law. However, it indicates that these eight knots cannot simultaneously satisfy Eqs. (8) and (9). Even if our data do support scaling laws for both p and C, the respective exponents cannot be equal, but rather will be in the ratio of about 3:4. As we show below, our data give greater support to Eq. (9).

IV. KNOT LOCALIZATION

Given a knotted ring polymer of N segments, we let N_K be the length of the shortest subsequence of the chain that still contains the knot. If $N_K \ll N$, then we say that the knot is localized. There is mounting evidence that knot localization is a general property in the sense that

$$\langle N_K\rangle/N \to 0 \quad \text{as} \quad N\to\infty.$$

TABLE II. Evidence for knot localization in several knots; N_K="knot length," or length of the shortest open sub-chain that is found in the same knot state as the complete chain.

	$\langle N_K\rangle$ N_K(min) N_K(max)							
N	**500**	**800**	**1000**	**1500**	**2000**	**10000**	b	t
3_1, swollen	166	219	264	368	359	848	6.3	0.54
	25	23	24	22	22	20		
	370	575	723	1330	1360	7486		
9_1, swollen	359	541	682	967	1197		1.5	0.88
	156	186	279	189	378			
	461	731	933	1416	1846			
"pretzel,"	403	616	756	1098	1415		1.4	0.91
swollen		317	411	387	503			
		777	948	1404	1895			
N	**500**	**1000**	**1500**	**2000**	**2500**			
3_1, theta	183	302	390	404	503		4.5	0.60
	22	23	27	25	32			
	409	271	1362	1596	1978			

This behavior is closely related to the behavior of paraknots, or ring chains that are restricted to pass through a sequence of slip links.[9–14] For example, consider an IR polymer of N segments required to visit sequentially each of the n vertices of a regular n-gon of side s, as in Fig. 2. We assume that the chain takes m_1 steps in passing from vertex 1 to vertex 2, m_2 steps in passing from vertex 2 to vertex 3, etc. We let $m_1, m_2, \ldots$ vary, subject to the constraint that $m_1 + m_2 + \cdots = N$. For s large the most probable state is $m_1 = m_2 = \cdots = m_n = N/n$. However, as s decreases, the system undergoes a symmetry-breaking transition, and for small s, the most probable state is one for which one of the $m_j's \approx N$, while all of the others are much smaller. In other words, the chain segregates into one large loop and $n-1$ small ones. Furthermore, we find that the entropy increases as $s \to 0$, so that these broken-symmetry configurations are the dominant states of the ensemble of variable s.[12] We believe that a similar process is responsible for knot localization in true knots.

Before finalizing the definition of N_K we must examine what we mean when we say that any given subsequence of the ring, which by definition is a noncyclic chain, is found in a given knot state. Formal topological considerations on knots always examine either closed paths, or at the very least, they examine nonclosed paths both of whose ends terminate on the surface of a simply connected object ("3-ball"). This latter approach provides a nonarbitrary definition of the knot state because we can join the two ends with a bridging path outside the 3-ball. We will apply the same concept here. An open path of length M on the lattice is specified through a list of its coordinates: $x_{\beta j}$, with $\beta \in \{1,2,3\}$ and $j \in \{1,2,\ldots,M\}$, where the $x_{\beta j}$'s are integers subject to the usual conditions of excluded volume and lattice-connectedness. Now, let L_β and H_β ("low" and "high") be the minimum and maximum values, respectively, of the $x_{\beta j}$'s extremized over all possible values of j, and let $[L_1, H_1]$ represent the set of integers between L_1 and H_1, inclusive. Then the set of lattice points given by $[L_1, H_1] \times [L_2, H_2] \times [L_3, H_3]$ defines the smallest possible rectangular box on the lattice which completely contains the chain. If both ends of the chain lie on the surface of this box, then we can unambiguously close the path by connecting the two ends with a bridging path lying entirely outside the box. We consider as ambiguous the situation in which either one or the other of the ends of the chain do not lie on the surface of this box, and therefore we consider its knot state to be indeterminate.[77] A chain in an indeterminate knot state is not in the same class as the unknot, rather its state is undefined. Our approach, therefore, is to consider all possible subchains extracted from the complete ring. If the knot state of any one is not indeterminate in the sense described above, we evaluate the knot state using our knot group procedure.[71] Finally, we define N_K as the length of the shortest subchain which still exhibits the same knot state as the complete ring.

Examining all possible subchains of a given ring is an expensive procedure, since each ring has approximately N^2 subchains. Therefore, knot localization for lattice SARs was investigated only for the knots 3_1, 9_1, and "pretzels;" and only for 3_1 for lattice θ-SARs. Table II and Fig. 3 give the values of $\langle N_K\rangle$ obtained. As is obvious in the figure, the N_K data can be represented by this power law,

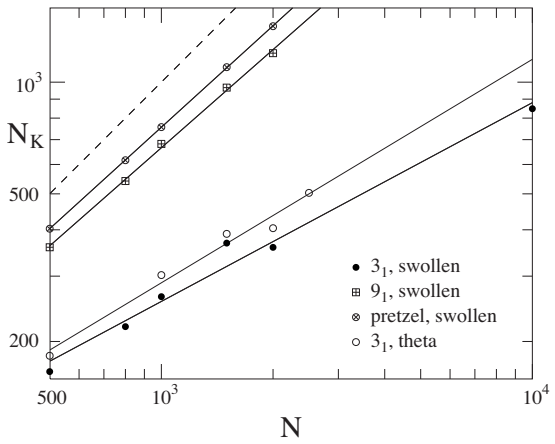

FIG. 3. Localization of knots in SARs in both swollen and theta states. $\langle N_K\rangle$ is the mean value of the shortest linear subchain of a ring that exhibits the same knot state as the complete ring. Extrapolation implies that $\langle N_K\rangle/N \to 0$, or that knots are localized in sufficiently large rings.

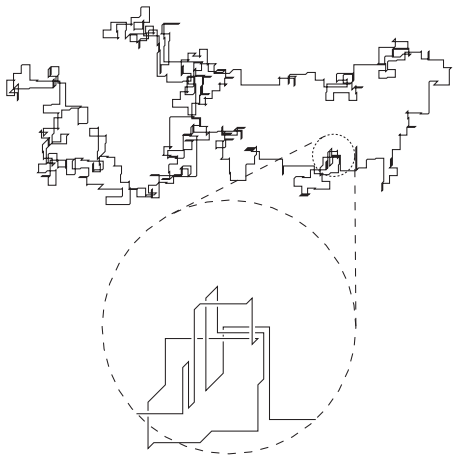

FIG. 4. Snapshot of a localized trefoil knot, $N=1000$. During annealing, the knot spontaneously and frequently localizes in a short section of the ring. Extrapolations imply that localization dominates in sufficiently large rings.

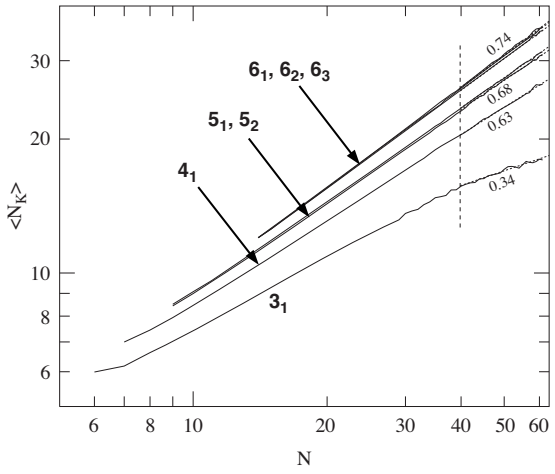

FIG. 5. Localization of knots in ideal, Gaussian rings. Effective exponents in the relationship $\langle N_K\rangle \sim N^t$ assume the indicated values in the interval $40 \leq N \leq 61$ for the seven knot states shown. Extrapolation again implies that $\langle N_K\rangle/N \to 0$, or that localization also occurs in IRs.

$$\langle N_K\rangle = bN^t, \tag{12}$$

with b and t values appearing in Table II. Note that $\langle N_K\rangle$ appears to increase with N, but less rapidly than N (since $t<1$), with the eventual result, therefore, that $\langle N_K\rangle/N \to 0$. Interestingly, with $t \approx 0.9$, $\langle N_K\rangle/N$ is decreasing for both 9_1 and the pretzel, but without data at higher N, it would not seem reasonable to call this direct evidence for localization of the two more complex knot types. For trefoils, however, knot-localization appears to be verified both for SARs and θ-SARs. Indeed, at $N=10\,000$ for the SAR trefoils, $\langle N_K\rangle/N$ is below 10%, while it is about 20% at $N=2500$ for θ-trefoils. A projection of a localized trefoil appears in Fig. 4. To further characterize the N_K distributions, Table II also gives $N_K(\min)$ and $N_K(\max)$, or the smallest and largest N_K values obtained over any given sample of constant N and knot type.

Marcone *et al.*[5] reported $t \approx 0.74$ for swollen SARs on the simple-cubic lattice for each of the three knot states 3_1, 4_1, and 5_1, and conjecture that the same value applies to all prime knots. Their results are therefore significantly different from the value we obtain: $t \approx 0.54$ for 3_1, and $t \approx 0.9$ for 9_1 and the pretzel. The discrepancy for both 9_1 and the pretzel can probably be explained away by recognizing that the more complex knots are not close to the asymptotic domain in which localization occurs. More difficult to explain is the discrepancy for the knot 3_1, but we note here that the two works use different definitions of N_K. Farago *et al.*[64] reported $t \approx 0.4$, for the knot 3_1 in bead models extended between two parallel impenetrable walls, but t was determined indirectly from force-extension data and not by direct determination of N_K, so again it is not clear that the two results are directly comparable.

Two conclusions about knot localization in SARs and θ-SARs become obvious. First, there is in every case a large difference between $N_K(\min)$ and $N_K(\max)$. So, even though localization is occurring, especially for trefoils, large fluctuations in N_K are common. Second, for all trefoil ensembles studied, we observe $N_K(\min) \cong n_{\min}=24$, suggesting that it is not uncommon, at the chain lengths studied, to observe optimally localized trefoils. (The structure in Fig. 4 is an example of a trefoil which, although somewhat longer than 24 units, is nevertheless localized.) This is especially significant when we recall that each sampling ensemble included only several hundred specimens. In other words, structures with $N_K(\min) \cong n_{\min}$ arise spontaneously and frequently during Monte Carlo annealing.[78] [We sometimes observe $N_K(\min) < n_{\min}$, which is possible for open knots, since a few segments are required for knot closure.]

Knot localization was also investigated for ideal Gaussian rings. We considered large ensembles of Gaussian chains at many values of $N \leq 61$. Once again, knot states of subchains were defined whenever both ends of a subchain terminate on a "3-ball," but in this case, the 3-ball was taken to be the smallest sphere that circumscribes the subchain, and N_K is defined as the length of the shortest subchain that has the same knot state as the complete ring. Figure 5 gives the N dependence of $\langle N_K\rangle$ for the seven simplest prime knots. Effective power-law exponents lie in the range 0.34–0.74 for N between 40 and 61 and for these particular knots. Just as before, we can expect $\langle N_K\rangle/N \to 0$ with increasing N. Figure 6 displays the distribution of N_K for several values of N for trefoil knots. According to Fig. 6, the most-probable N_K is near 10 for all values of N, and the distribution functions at $N=48$ and at $N=60$ are practically identical.

Our results obviously present a strong case for localization of trefoils under good-solvent, theta-solvent, and ideal conditions. By extension, knot localization is a reasonable expectation for all knot classes, although our results for 9_1 and the pretzel are not at sufficiently large N to constitute direct evidence. Furthermore, since it appears that $\langle N_K\rangle/N \to 0$ generally, it must be true that $R_g \to AN^\nu$ with A and ν being independent of knot type, and that such universality occurs under good-solvent, theta-solvent, and ideal-chain conditions.

V. R_g DATA

Log-log plots displaying R_g as a function of N for all the knots appearing in Fig. 1, and under both swollen and theta

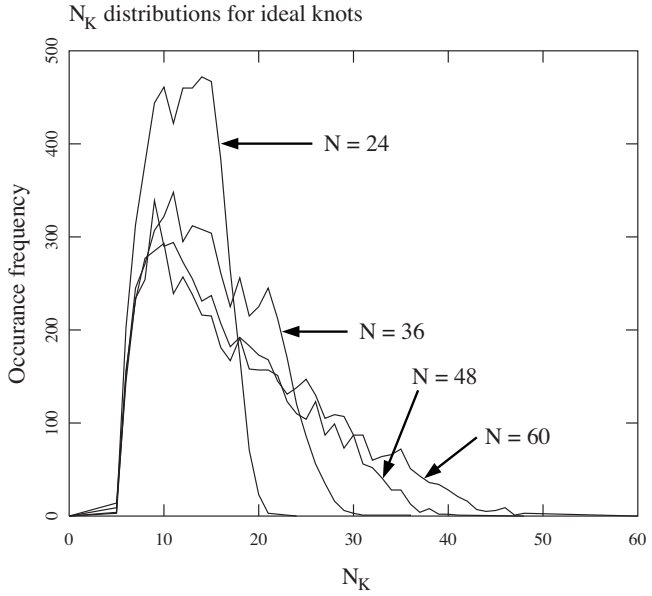

FIG. 6. Distribution of trefoil knot lengths in ideal, Gaussian rings. The most-probable knot length is about 10 and independent of N.

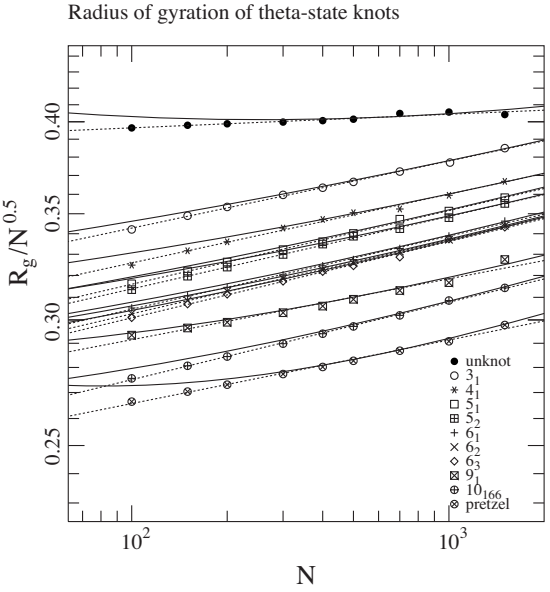

FIG. 8. Radius-of-gyration scaling for self-avoiding, theta-state knots. Dashed curves are the least-squares lines. Solid curves are the least-squares fits to Eq. (6).

conditions, are shown in Figs. 7 and 8, respectively. To emphasize discrepancies between respective effective exponents, we actually display $R_g/N^{0.588}$ or $R_g/N^{0.5}$ in these figures. Normalization in this way makes the dependence appearing on the right-hand side of Eq. (5) appear flat, and therefore lets us observe clearly that the inequality in Eq. (5) is always satisfied by the data. The best least-squares lines appear as dashed lines in these figures. The log-log curves are practically linear. However, the linear-least-squares residuals in the log-log data [defined as the difference between $\log(R_g/N^{\nu})$ and the least-squares line] although noisy, show enough systematic dependence on N for us to be confident in reporting that the curves for swollen and theta knots are slightly curved, being concave up and down, respectively.

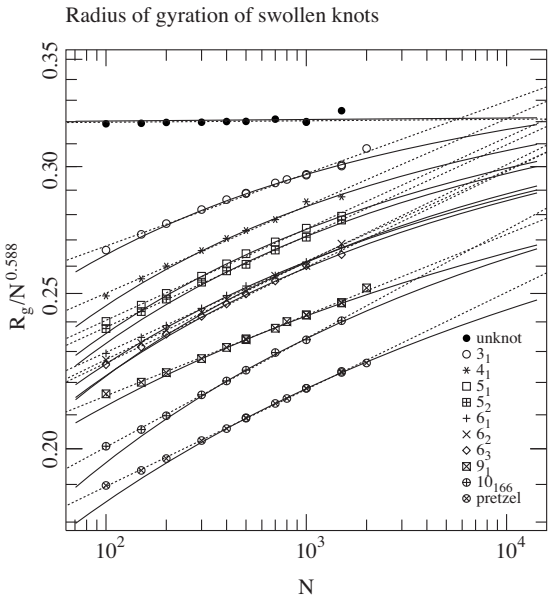

FIG. 7. Radius-of-gyration scaling for self-avoiding, swollen knots. Dashed curves are the least-squares lines. Solid curves are the least-squares fits to Eq. (6).

The effective exponents and prefactors given by the least-squares lines and computed over the interval $100 \leq N \leq 2000$ are assembled in Table III. We note that the effective exponents for the unknot, 0.589 and 0.509, are in good agreement with Eqs. (1), which, as previously stated, can be expected because the respective unrestricted ensembles are unknot dominant at these values of N. Furthermore, the effective metric exponents for knots are about 0.64 when swollen and are around 0.54 for theta conditions, or about 0.04 to 0.06 larger than the values obtained for unknots. There is also a difference of about 0.1 between the metric exponents for swollen and theta-chains.

We intuitively expect R_g to decrease with knot complexity, and for the purposes of this paper, we will accept this as a given. Then we can expect that the curves in Figs. 7 and 8 will never cross. This noncrossing requirement indicates one important thing: The curves may appear to be more or less flat, but nevertheless, they are not in an asymptotic domain. At least some of the curves must bend somewhere beyond $N > 2000$ to avoid any crossing.

TABLE III. Effective metric exponents for swollen and theta knots. Slopes of the least-squares lines appearing in Figs. 7 and 8 for $100 \leq N \leq 2000$.

	ν_{SW}	ν_θ	$\nu_{SW} - \nu_\theta$
Unknot	0.589	0.509	0.080
3_1	0.633	0.542	0.091
4_1	0.642	0.543	0.099
5_1	0.645	0.546	0.099
5_2	0.645	0.546	0.099
6_1	0.645	0.546	0.099
6_2	0.649	0.547	0.102
6_3	0.648	0.548	0.100
9_1	0.638	0.538	0.100
10_{166}	0.656	0.549	0.107
"Pretzel"	0.649	0.540	0.109

TABLE IV. Least-squares fits of Eq. (6) for swollen knots.

	A	ν
All knot states	0.348	0.588
	B	Δ
Unknot	−0.083	0.011
3_1	−0.602	0.204
4_1	−0.696	0.191
5_1	−0.704	0.174
5_2	−0.714	0.170
6_1	−0.674	0.145
6_2	−0.733	0.157
6_3	−0.700	0.147
9_1	−0.616	0.102
10_{166}	−0.753	0.121
"Pretzel"	−0.713	0.094

As already pointed out, a direct consequence of the knot-localization property is that all knots scale asymptotically as unknots of length $N-N_K \cong N$, which in turn indicates that the asymptotic metric exponent ν and amplitude A are independent of knot state. To test this, we have performed a least-squares fit of our data to Eq. (6) under the following assumptions. (1) The amplitude A and the exponent ν are universal for all knots of given solvent quality. Therefore, although their respective values were permitted to adjust during the fit, the same values of A and ν were assigned to all knots of a given solvent quality. (2) The coefficient B and the exponent Δ were permitted to adjust separately for each knot type, subject to the constraint $\Delta \geq 0$. (3) Consistent with the fact that Eq. (6) only contains two leading terms, and therefore is only valid at larger N, we have weighted points at $N > 10^{2.5}$ and points at $N < 10^{2.5}$ differently, with relative weights 1 and 0.1, respectively. Results of these fits are given in Tables IV and V for swollen and theta-chains, respectively, and the best-fit results are also shown as solid curves in Figs. 7 and 8. The fit is good enough, especially at higher N, that it is reasonable to assert that our data are consistent with both A and ν being independent of knot state. The ν exponents that give the optimal agreement with our data are 0.588 and 0.579 for swollen and theta knots, respectively. Therefore, our data display a plausible extrapolation that is consistent with the assertion that ν_{SAR} is the correct asymptotic exponent. This result could not have been anticipated from the apparent exponents listed in Table III, which typically are significantly different from ν_{SAR}. The phenomenon of knot localization requires a single asymptotic exponent for all knot types, and when we impose that constraint on our fit, our data automatically select values near ν_{SAR}.

TABLE V. Least-squares fits of Eq. (6) for theta-state knots.

	A	ν
All knot states	0.157	0.579
	B	Δ
Unknot	1.974	0.202
3_1	0.963	0.130
4_1	0.917	0.150
5_1	0.789	0.142
5_2	0.833	0.156
6_1	0.748	0.159
6_2	0.744	0.162
6_3	0.708	0.157
9_1	0.882	0.234
10_{166}	0.708	0.240
"Pretzel"	1.504	0.433

The least-squares fits display one disquieting aspect. At least some of the curves for knots, when extrapolated to very large N, are observed to intersect the respective curves for the unknot, and as already mentioned, we believe this to be implausible. When an additional constraint to disallow such crossings was imposed, the quality of the fit deteriorated significantly. One possible explanation of the crossings of the least-squares curves is that we are so far from the asymptotic domain that to obtain truly well-behaved fits, it would require additional correction terms in Eq. (6).

Figure 9 examines the relationship between R_g and p at each of the N values studied. (Similar plots for the dependence of R_g on C were prepared, but are not presented here.) We again note the existence of effective scaling laws, and we report in Table VI the effective exponents. The effective exponents relative to p are in the vicinity of $-4/15 \cong -0.267$ as predicted by Grosberg *et al.*[2] Lai *et al.*[56] reach a similar conclusion for a bead-spring polymer model. The Quake prediction of $C^{-4/15}$ is not supported, since, as already stated, Eq. (11) implies that the two predictions are inconsistent. We have already noted that the knot-localization phenomenon is inconsistent with the basic assumption of the Grosberg–Feigel–Rabin scaling law. Therefore, it is conceivable that $p^{-4/15}$ is a characteristic of an intermediate chain-length regime. However, if knots eventually become localized at large enough N, then, as already mentioned, we expect R_g to become independent of knot type and therefore of p in the asymptotic limit. Indeed, the trend in the effective exponent, gradually decreasing as N increases, is consistent with this conclusion.

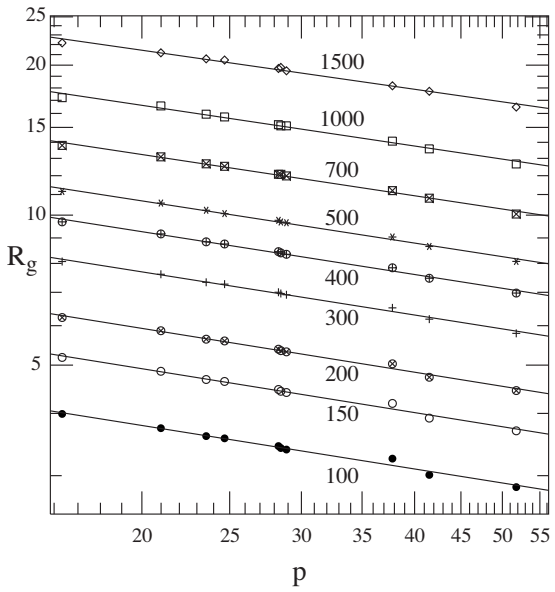

FIG. 9. Scaling of radius of gyration of swollen knots with knot complexity, measured as p=length:diameter ratio (or "rope-length") of the maximally inflated conformation. Values of N are indicated.

TABLE VI. Effective exponents for the dependence of R_g on p and C.

N	R_g vs p	R_g vs C
100	−0.290	−0.211
150	−0.293	−0.213
200	−0.292	−0.212
300	−0.287	−0.209
400	−0.286	−0.208
500	−0.281	−0.205
700	−0.275	−0.200
1000	−0.271	−0.198
1500	−0.260	−0.190

VI. CONCLUSIONS

We accept as obvious the premise that knot size, as measured by R_g, must be negatively correlated with knot complexity. This implies that the curves in Fig. 7 and 8, when extrapolated to larger N, must bend in order to avoid any crossings. This implies that our data have not reached an asymptotic domain. Therefore, many of our predictions concerning the long-chain behavior of ring polymers restricted to specific knot states are based on extrapolations to large N and are conjectural. However, our data support the following assertions for knots in good and theta solvents.

(1) Extrapolation of our results to large N indicates that knot localization is anticipated for sufficiently long lattice SARs, lattice θ-SARs, and ideal Gaussian rings.
(2) Effective metric exponents for SAR and θ-SAR unknots are near ν_{SAR} and ν_{IR}, respectively, over the chain-length range studied here. This behavior is to be expected because the respective ensembles that are unrestricted by knot type are unknot-dominant. Effective exponents for SAR and θ-SAR knots (as opposed to unknots) are near 0.65 and 0.55, respectively, again over the chain-length range considered here. This behavior also should come as no surprise, since it is consistent with the inequality of Eq. (5).
(3) Because of knot localization, it is reasonable to anticipate that all knots and unknots will eventually cross over to an asymptotic domain for which $R_g \rightarrow AN^{\nu}$, with the same A and ν for all knot types.
(4) Our data are consistent with extrapolations that give $A \cong 0.35$ and $A \cong 0.16$ for SARs and θ-SARs, respectively. The same extrapolations give $\nu \cong 0.59$ and $\nu \cong 0.58$, respectively. Therefore, our results are consistent with the widely stated assertions for knotted rings, namely, that $\nu_{\mathrm{SAR}} \cong 0.588$ is the correct asymptotic exponent for both SARs and IRs that are restricted to any particular knot state. These extrapolations were determined by allowing the values of ν to adjust, and it is probably significant that the fitting procedure automatically selected values near ν_{SAR}.
(5) If both SARs and θ-SARs are to have the same asymptotic exponent of 0.588, then the unknot curve in Fig. 7 should remain horizontal, while the unknot curve in Fig. 8 should bend upward. A reviewer has suggested that a more consistent explanation is that extrapolations on both sets of data should behave similarly, so that ν_{IR} would be the correct asymptotic exponent for either IRs or θ-SARs when restricted to a given knot state. In the absence of additional accurate data at larger N, we prefer not to judge between these two alternative viewpoints.
(6) In an intermediate range of chain lengths, before knot localization becomes important, we observe the scaling laws $R_g \sim p^{-0.27}$ and $R_g \sim C^{-0.20}$ for the good solvent domain, at least for the knots examined here. This is in reasonable agreement with Eq. (9) but not Eq. (8). $(4/15 \cong 0.267)$. Indeed, because we do not observe $p \sim C$, Eqs. (8) and (9) are incompatible. The $R_g \sim p^{-0.27}$ scaling law is based on assumptions that are inconsistent with knot localization and therefore is not expected to extend to larger N. The observed N-dependence of the effective exponent is consistent with this expectation.

ACKNOWLEDGMENTS

We acknowledge the assistance of Professor Piotr Pieranski and Professor Sylvester Przybyl, Poznan University of Technology, Poznan, Poland, and of Professor Eric J. Rawdon, University of St. Thomas, St. Paul, Minnesota, USA in providing maximally-inflated conformations of knots 10_{166} and $(-3,5,7)$-pretzel.

[1] According to this study and others which we cite below, it seems likely that knots in long chains are localized. Therefore, unlike typical global properties, some knot properties may be sensitive to the distinction between ideal and theta chains.
[2] A. Yu. Grosberg, A. Feigel, and Y. Rabin, Phys. Rev. E **54**, 6618 (1996).
[3] E. Guitter and E. Orlandini, J. Phys. A **32**, 1359 (1999).
[4] V. Katritch, W. K. Olson, A. Vologodskii, J. Dubochet, and A. Stasiak, Phys. Rev. E **61**, 5545 (2000).
[5] B. Marcone, E. Orlandini, A. L. Stella, and F. Zonta, J. Phys. A **38**, L15 (2005).
[6] Y. Kantor, Pramana, J. Phys. **64**, 1011 (2005).
[7] E. Ercolini, F. Valle, J. Adamcik, G. Witz, R. Metzler, P. De Los Rios, J. Roca, and G. Dietler, Phys. Rev. Lett. **98**, 058102 (2007).
[8] E. Orlandini and S. G. Whittington, Rev. Mod. Phys. **79**, 611 (2007).
[9] J. Rieger, Polym. Bull. **18**, 343 (1987).
[10] J. Rieger, J. Phys. A **21**, L1085 (1988).
[11] J. Rieger, Macromolecules **22**, 4540 (1989).
[12] M. L. Mansfield, Macromolecules **24**, 3395 (1991).
[13] R. Metzler, A. Hanke, P. G. Dommersnes, Y. Kantor, and M. Kardar, Phys. Rev. E **65**, 061103 (2002).
[14] R. Metzler, Y. Kantor, and M. Kardar, Phys. Rev. E **66**, 022102 (2002).
[15] E. Orlandini, A. L. Stella, and C. Vanderzande, Phys. Rev. E **68**, 031804 (2003).
[16] H. L. Frisch and E. Wasserman, J. Am. Chem. Soc. **83**, 3789 (1961).
[17] M. Delbrück, Proc. Symp. Appl. Math. **14**, 55 (1962).
[18] D. W. Sumners and S. G. Whittington, J. Phys. A **21**, 1689 (1988).
[19] C. E. Soteros, D. W. Sumner, and S. G. Whittington, Math. Proc. Cambridge Philos. Soc. **111**, 75 (1992).
[20] E. J. Janse van Rensburg, D. A. W. Sumners, E. Wasserman, and S. G. Whittington, J. Phys. A **25**, 6557 (1992).
[21] Y. Diao, N. Pippenger, and D. W. Sumners, J. Knot Theory Ramif. **3**, 419 (1994).
[22] Y. Diao, J. Knot Theory Ramif. **4**, 189 (1995).
[23] Y. Diao, J. C. Nardo, and Y. Sun, J. Knot Theory Ramif. **10**, 597 (2001).
[24] G. Ten Brinke and G. Hadziioannou, Macromolecules **20**, 480 (1987).
[25] E. J. Janse van Rensburg and S. G. Whittington, J. Phys. A **23**, 3573 (1990).
[26] K. Koniaris and M. Muthukumar, J. Chem. Phys. **95**, 2873 (1991).
[27] K. Koniaris and M. Muthukumar, Phys. Rev. Lett. **66**, 2211 (1991).
[28] T. Deguchi and K. Tsurusaki, J. Phys. Soc. Jpn. **62**, 1411 (1993).

[29] T. Deguchi and K. Tsurusaki, J. Knot Theory Ramif. **3**, 321 (1994).
[30] M. C. Tesi, E. J. Janse van Rensburg, E. Orlandini, D. W. Sumners, and S. G. Whittington, Phys. Rev. E **49**, 868 (1994).
[31] K. Tsurusaki and T. Deguchi, J. Phys. Soc. Jpn. **64**, 1506 (1995).
[32] T. Deguchi and K. Tsurusaki, Phys. Rev. E **55**, 6245 (1997).
[33] E. Orlandini, M. C. Tesi, E. J. Janse van Rensburg, and S. G. Whittington, J. Phys. A **31**, 5953 (1998).
[34] M. K. Shimamura and T. Deguchi, Phys. Lett. A **274**, 184 (2000).
[35] A. Dobay, P.-E. Sottas, J. Dubochet, and A. Stasiak, Lett. Math. Phys. **55**, 239 (2001).
[36] A. Yao, H. Matsuda, H. Tsukahara, M. K. Shimamura, and T. Deguchi, J. Phys. A **34**, 7563 (2001).
[37] M.K. Shimamura, T. Deguchi, Phys. Rev. E **66**, 040801(R) (2002).
[38] K. Millett, A. Dobay, and A. Stasiak, Macromolecules **38**, 601 (2005).
[39] P. Virnau, Y. Kantor, and M. Karder, J. Am. Chem. Soc. **127**, 15102 (2005).
[40] N. T. Moore and A. Y. Grosberg, J. Phys. A **39**, 9081 (2006).
[41] E. Orlandini, M. C. Tesi, and S. G. Whittington, J. Phys. A **38**, L795 (2005).
[42] M. L. Mansfield, J. Chem. Phys. **127**, 244902 (2007).
[43] M. L. Mansfield, Macromolecules **27**, 5924 (1994).
[44] R. Lua, A. L. Borovinskiy, and A. Yu. Grosberg, Polymer **45**, 717 (2004).
[45] M. L. Mansfield, J. Chem. Phys. **125**, 154103 (2006).
[46] A. Stasiak, J. Dubochet, V. Katritch, and P. Pieranski, in *Ideal Knots*, edited by A. Stasiak, V. Katritch, and L. H. Kauffman (World Scientific, New York, 1999), pp. 1–19.
[47] Obviously, this terminology engenders the risk of confusion: Polymer scientists employ the term "ideal" to refer to polymer models without excluded volume. In this and the companion paper, we obviously will have occasion to refer to "ideal knots" in both connotations. Therefore, we will let the term ideal refer to the absence of excluded volume interactions, and maximally inflated refer to the knot conformation satisfying the criterion that L/d is at its global minimum.
[48] V. Katritch, J. Bednar, D. Michoud, R. G. Scharein, J. Dubochet, and A. Stasiak, Nature (London) **384**, 142 (1996).
[49] P. Pieranski, Poznan University of Technology, Poznan, Poland, fizyka.phys.put.poznan.pl/~pieransk/.
[50] E. J. Rawdon, private communication (2009).
[51] S. Przybyl, private communication (2009).
[52] A. Dobay, J. Dubochet, K. Millett, P.-E. Sottas, and A. Stasiak, Proc. Natl. Acad. Sci. U.S.A. **100**, 5611 (2003).
[53] C. C. Adams, *The Knot Book: An Elementary Introduction to the Mathematical Theory of Knots* (W.H. Freeman, New York, 1994).
[54] E. J. Janse van Rensburg and S. G. Whittington, J. Phys. A **24**, 3935 (1991).
[55] S. R. Quake, Phys. Rev. Lett. **73**, 3317 (1994).
[56] P.-Y. Lai, Y.-J. Sheng, and H.-K. Tsao, Physica A **281**, 381 (2000).
[57] J. M. Deutsch, Phys. Rev. E **59**, R2539 (1999).
[58] A. Yu. Grosberg, Phys. Rev. Lett. **85**, 3858 (2000).
[59] N. T. Moore, R. C. Lua, and A. V. Grosberg, Proc. Natl. Acad. Sci. U.S.A. **101**, 13431 (2004).
[60] N. T. Moore and A. Y. Grosberg, Phys. Rev. E **72**, 061803 (2005).
[61] M. K. Shimamura and T. Deguchi, Phys. Rev. E **64**, 020801(R), 2001.
[62] M. K. Shimamura and T. Deguchi, Phys. Rev. E **65**, 051802 (2002).
[63] M. K. Shimamura and T. Deguchi, J. Phys. A **35**, 102 (2002).
[64] O. Farago, Y. Kantor, and M. Kardar, Europhys. Lett. **60**, 53 (2002).
[65] M. Doi and S. F. Edwards, *The Theory of Polymer Dynamics* (Oxford University Press, Oxford, 1986).
[66] A. N. Rissanou, S. H. Anastasiadis, and I. A. Bitsanis, J. Polym. Sci., Part B: Polym. Phys. **44**, 3651 (2006).
[67] B. Berg and D. Foerster, Phys. Lett. B **106**, 323 (1981).
[68] C. Aragão de Carvalho, J. Phys. (Paris) **44**, 323 (1983).
[69] C. Aragao de Carvalho, S. Caracciolo, and J. Frohlich, Nucl. Phys. B **215**, 209 (1983).
[70] E. J. Jense van Rensburg and S. G. Whittington, J. Phys. A **24**, 5553 (1991).
[71] M. L. Mansfield, J. Chem. Phys. **127**, 244901 (2007).
[72] R. H. Crowell and R. H. Fox, *Introduction to Knot Theory* (Ginn & Co., Boston, 1963).
[73] D. Rolfsen, *Knots and Links* (Publish or Perish, Berkeley, CA, 1976).
[74] Y. Diao, J. Knot Theory Ramif. **2**, 413 (1993).
[75] E. J. Janse van Rensburg and S. D. Promislow, J. Knot Theory Ramif. **4**, 115 (1995).
[76] R. Scharein, K. Ishihara, J. Arsuaga, Y. Diao, K. Shimokawa, and M. Vazquez, J. Phys. A: Math. Theor. **42**, 475006 (2009).
[77] The notion of indeterminate knot state is meant to represent a situation which could be encountered with actual ropes or strings. Imagine two tangled ropes. In one case, at least one end of the rope is embedded in the tangle, while in the other, both ends are free and clear of the tangled portion of the rope. All reasonable individuals would agree that the latter rope has a definite knot state, but they might not agree about the definition of the knot state in the former case. To avoid any subjectivity or arbitrariness, we choose to leave the knot state undefined in the former situation.
[78] It would not be inappropriate to refer to the localized knots discussed here as "tight knots." However, we point out that DeGennes has used the term "tight knot," [P.-G. DeGennes, Macromolecules **17**, 703 (1984)] in what we believe is a different context. He considered knots in polymers that were "atomically tight" (our neologism, not his), or knots tightened by an externally applied tension sufficient to generate a unique conformation that is essentially the polymeric equivalent of the maximally inflated knot. Knot localization, in the present context, should be thought of as arising from an internal tension generated by the excluded volume interaction, but we do not envision that this tension is strong enough to force the knot into a unique conformation. He speculated that a sufficiently strong tension might create stable tight knots. Molecular dynamics calculations indicate, however, that room-temperature thermal motion is adequate to loosen even the tightest knots, and that a knotted polymer strand breaks under tension before forming a stable tight knot [M. L. Mansfield, *ibid.* **31**, 4030 (1998)].